# Light Higgs Boson Searches within NMSSM

Dharmender

on behalf of NMSSM analysis group





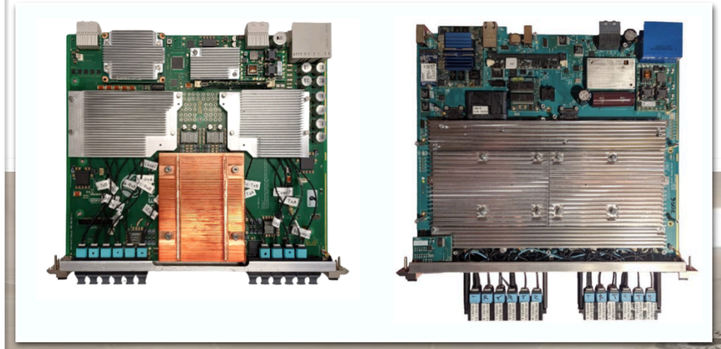


**Higgs @ GGI, Florence, Italy** : 28 Sept - 2 Oct 2026

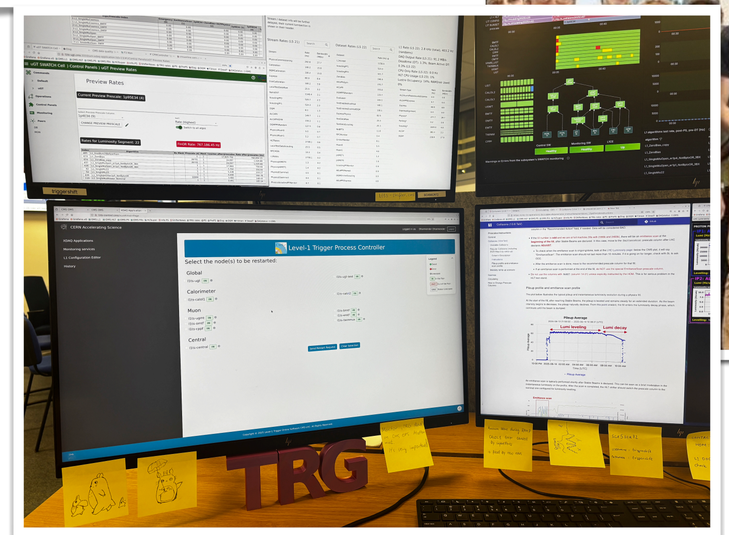
# A bit about me










CMS - Level 1 Trigger

- Jets
- Burn-in tests
- Online Software
- Light Higgs Search

# A bit about me















@harmender

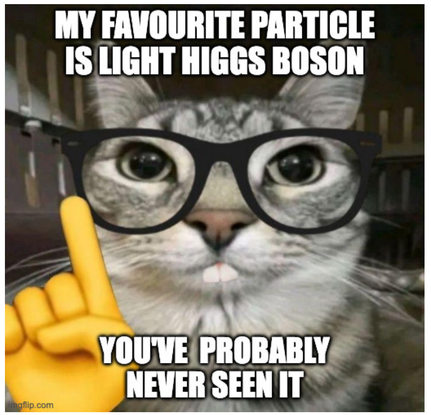
# Introduction

## Search for low-mass Higgs bosons decaying to bb




- Many BSM theories predicts more than one Higgs[1,2]
- Less-explored signature may still evade current limits[3,4]
- Analysis focuses on light Higgs searches with low missing transverse energy[5]

# Run-2 Analysis Paper




Eur. Phys. J. C (2023) 83:571
https://doi.org/10.1140/epjc/s10052-023-11581-0

THE EUROPEAN PHYSICAL JOURNAL C

Check for updates

Regular Article - Experimental Physics

## Search for light Higgs bosons from supersymmetric cascade decays in pp collisions at $\sqrt{s} = 13$ TeV

**CMS Collaboration***

CERN, 1211 Geneva 23, Switzerland

Received: 28 April 2022 / Accepted: 1 July 2022 / Published online: 6 July 2023
© CERN for the benefit of the CMS collaboration 2023

138fb-1

mH = [30, 125] GeV

Full Run 2 CMS Data

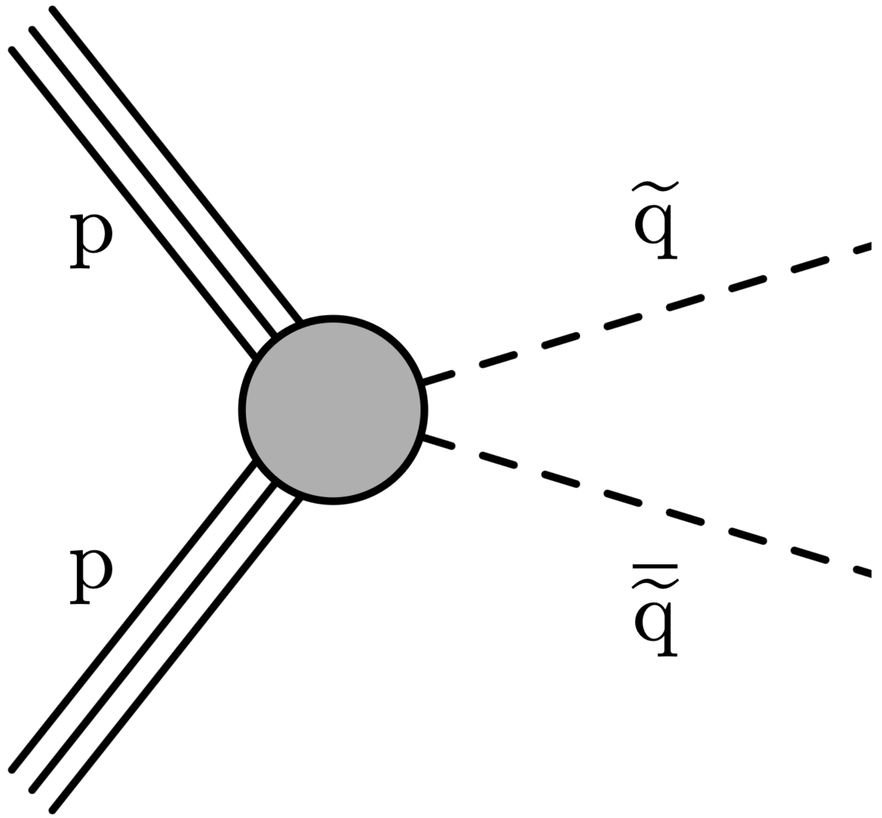
**Abstract** A search is reported for pairs of light Higgs bosons ($H_1$) produced in supersymmetric cascade decays in final states with small missing transverse momentum. A data set of LHC pp collisions collected with the CMS detector at $\sqrt{s} = 13$ TeV and corresponding to an integrated luminosity of 138 $fb^{-1}$ is used. The search targets events where both $H_1$ bosons decay into $b\bar{b}$ pairs that are reconstructed as large-radius jets using substructure techniques. No evidence is found for an excess of events beyond the background expectations of the standard model (SM). Results from the search are interpreted in the next-to-minimal supersymmetric extension of the SM, where a "singlino" of small mass leads to squark and gluino cascade decays that can pro-

other SUSY particles, suppressing direct squark or gluino decays to the $\tilde{\chi}_S^0$. Squarks and gluinos decay via the next-to-LSP $\tilde{\chi}_2^0$ into a $\tilde{\chi}_S^0$ and a Higgs, Z, or W boson [10,11]. The case of a singlet-like *CP*-even $H_1$, shown in Fig. 1, is the focus of this search. When the $\tilde{\chi}_S^0$ has a far smaller mass than the $H_1$ and the phase space for the decay $\tilde{\chi}_2^0 \to H_1 + \tilde{\chi}_S^0$ is small, the $H_1$ carries much larger momentum than the $\tilde{\chi}_S^0$. In such $p_T^{miss}$-suppressed scenarios, the key signature for the pair production of squarks and gluinos is a pair of Lorentz-boosted $H_1$ bosons.

This search targets events with two highly boosted $H_1$ bosons that decay into $b\bar{b}$ pairs that are reconstructed as large-radius jets using substructure techniques. This is the

# Signal Model

Lower susy mass => less Higgs boost => large angular separation ΔR(bb)

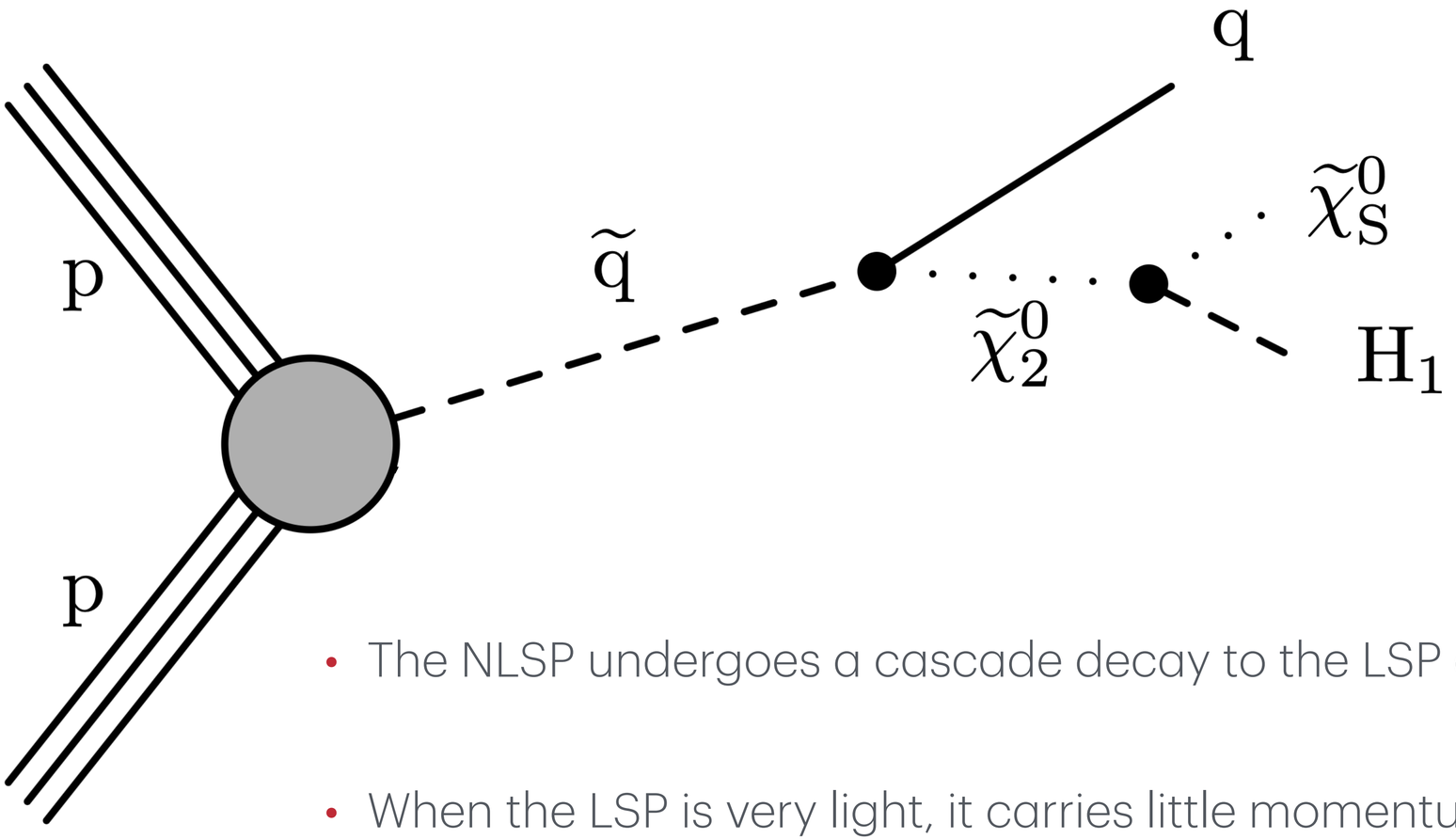



**$M_{susy}$ > 1200 GeV**

| $m_{\mathrm{SUSY}}$ [GeV] | $\sigma(pp \to \tilde{q}\tilde{q}, \tilde{q}\tilde{g}, \tilde{g}\tilde{g})$ [fb] | Uncertainty |
|---|---|---|
| 1200 | 582.3 | 8% |
| 1400 | 194.1 | 9% |
| 1600 | 69.71 | 9% |
| 1800 | 26.29 | 10% |
| 2000 | 10.29 | 11% |
| 2200 | 4.114 | 13% |
| 2400 | 1.668 | 14% |
| 2600 | 0.6792 | 16% |
| 2800 | 0.2765 | 18% |
| 3000 | 0.1117 | 21% |
| 3200 | 0.04512 | 24% |

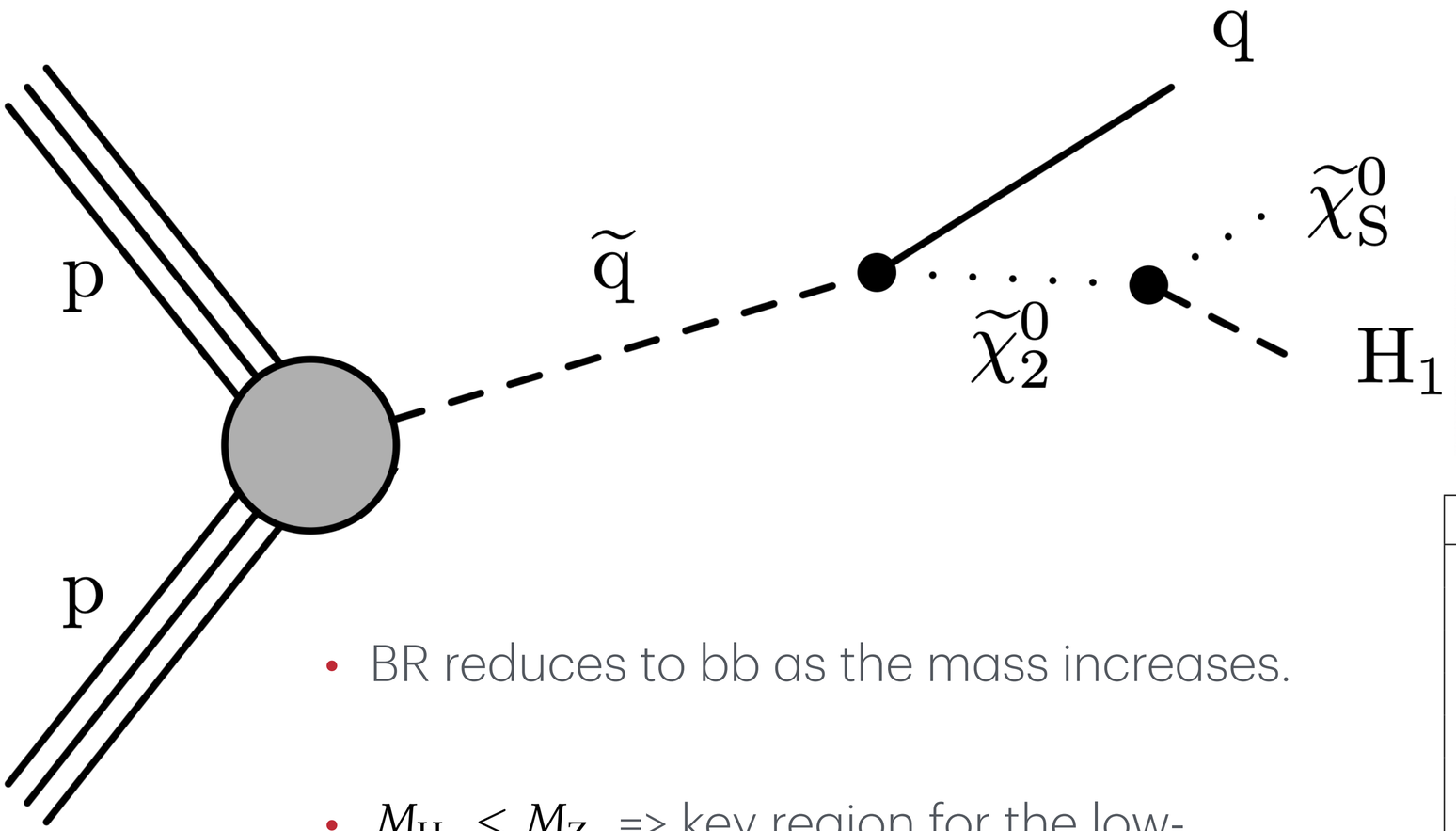
**Table 1:** Cross-section for different $M^{susy}$

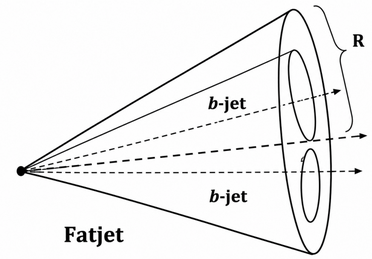
# Signal Model




- The NLSP undergoes a cascade decay to the LSP and a Higgs boson;
- When the LSP is very light, it carries little momentum, so the Higgs boson takes most of the boost.

# Signal Model




- BR reduces to bb as the mass increases.
- $M_{H_1} < M_Z$ => key region for the low-missing-momentum hadronic signature.

| $M_{H_1}$ | BR ($H_1 \to b\bar{b}$) |
|---|---|
| 30 GeV | 0.868 |
| 35 GeV | 0.867 |
| 40 GeV | 0.865 |
| 50 GeV | 0.858 |
| 60 GeV | 0.850 |
| 70 GeV | 0.840 |
| 80 GeV | 0.829 |
| 90 GeV | 0.816 |
| 100 GeV | 0.795 |
| 110 GeV | 0.749 |
| 125 GeV | 0.581 |

# Signal Model

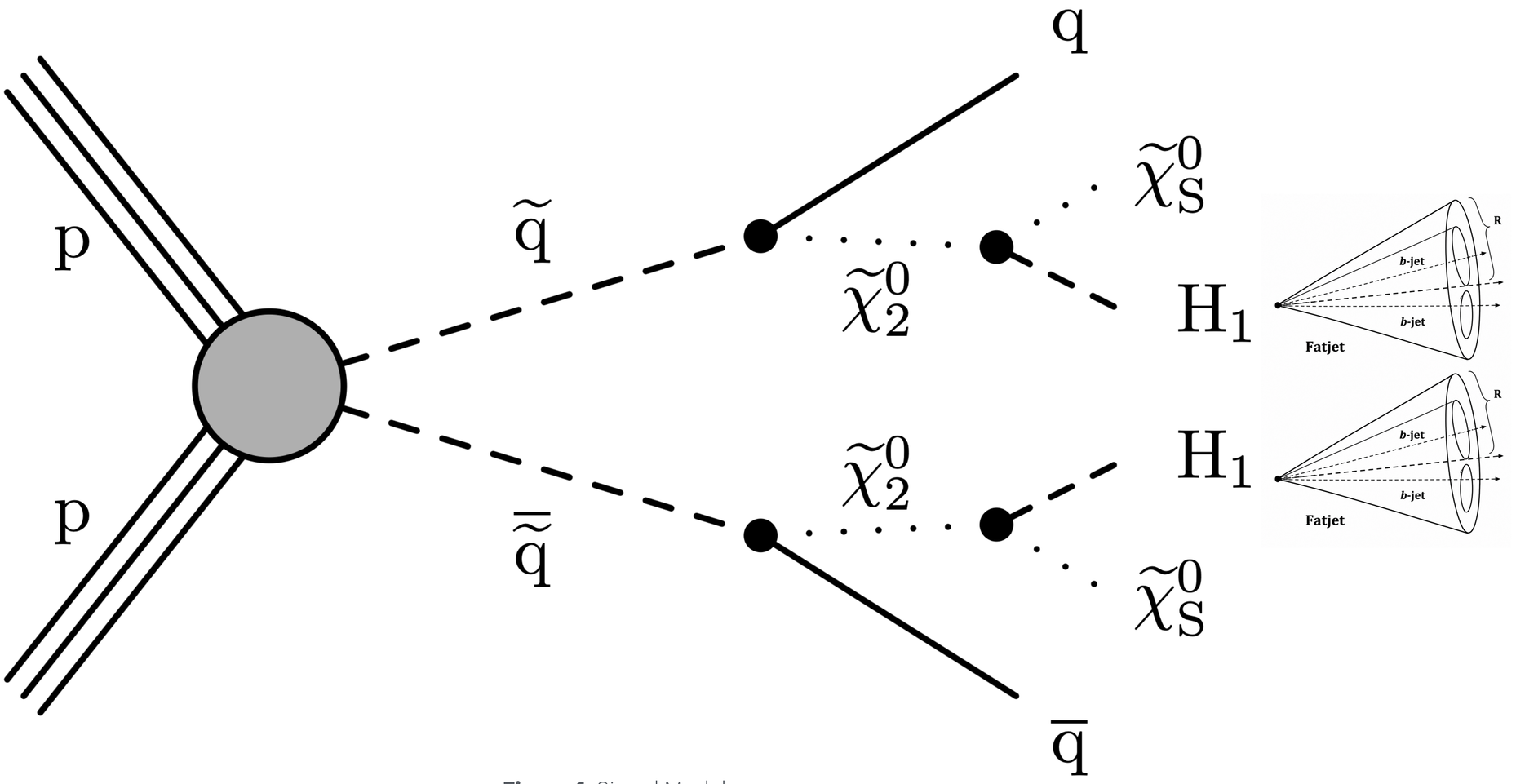
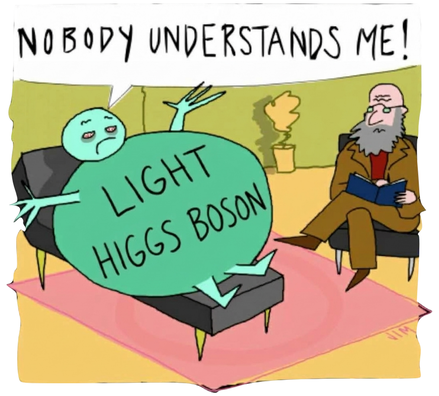
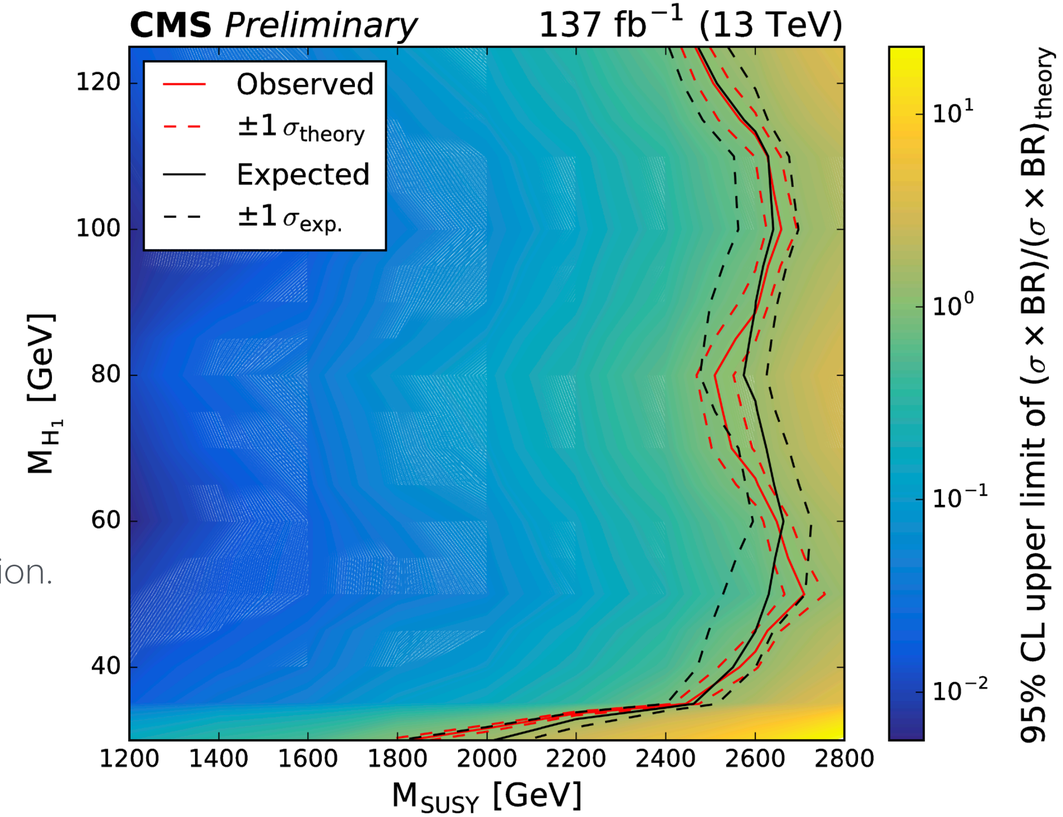



**Figure 1:** Signal Model.

# Run-2 Paper: Summary




- No significant excess observed.
- Data consistent with SM expectation.
- Limits set on low-mass Higgs production.




## Main Limitation

- SoftDrop grooming removes part of the jet energy, could be too aggressive.
- Mass resolution degrades.
- Acceptance rapidly decreases, because of lower boundary of the mass Grid.

**Figure 2:** The observed 95% CL upper limit of (σ x BR)/(σ x BR)theory (indicated by the colour scale) as a function of H1 and MSUSY . The solid red (black) line delineates the observed (median expected) excluded region. The dashed red (black) line delineates the observed (expected) excluded regions with ±1σ in theoretical (experimental) uncertainty

# Run-3 opportunities

## GloPart Tagger[6]

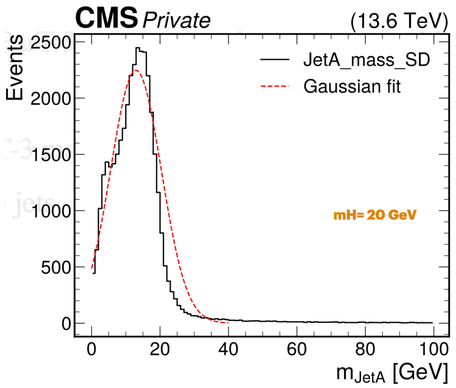
- particle-level information
- transformer architecture
- simultaneous flavour and mass information

## Expected improvements:

- better jet tagging
- improved mass reconstruction
- access to lower mass resonances

- Larger dataset.
- Improved reconstruction.
- New ML-based jet taggers and mass regressions.

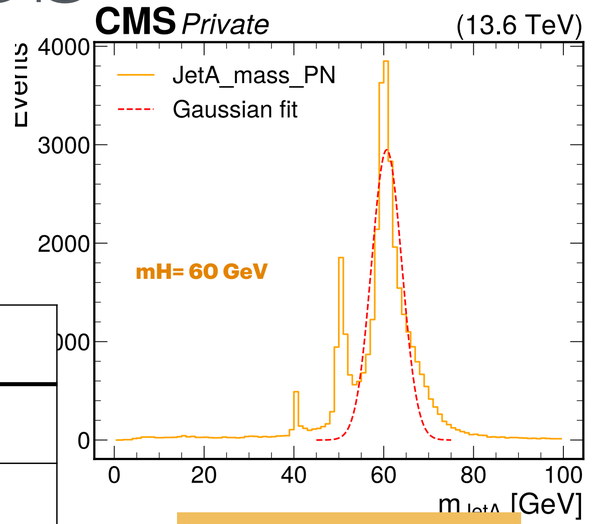
# Available Mass variables




SoftDrop

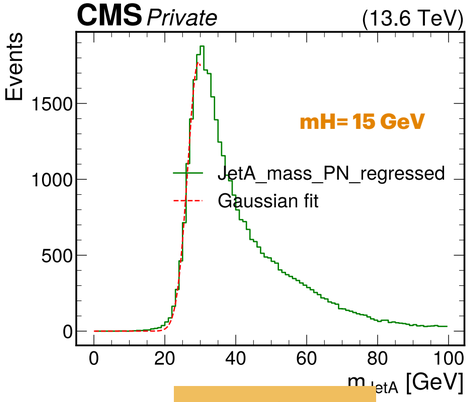
| Variable | Description |
|---|---|
| mSoftDrop | SoftDrop + PUPPI |
| ParticleNet Legacy Mass | Run-2 mass regression |
| ParticleNet Mass Corr | Modern ParticleNet mass regression |
| GloParT Generic | generic jet mass regression |
| GloParT 2-prong | resonance-optimized mass regression |

Final choice




Particle Net Legacy

- Final choice: Glopart:2p
- Better for bb,cc or 2 prong decays, giving better results for our search (H->bb decays)[6]




Particle Net

# Mass variable choice

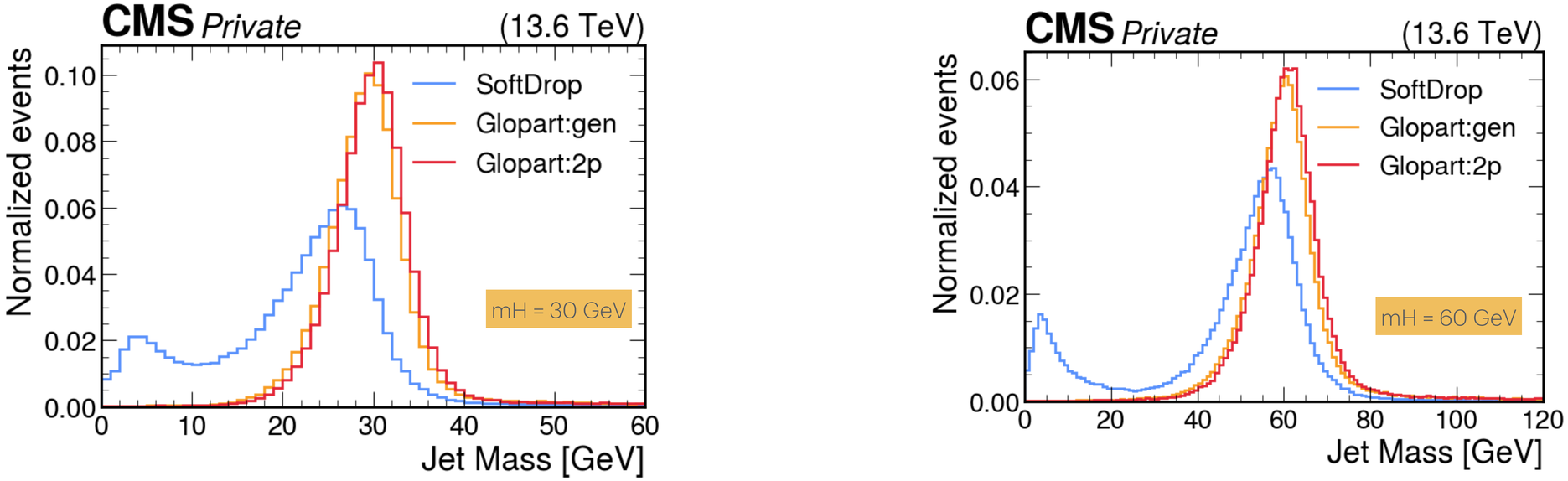



**Figure 4:** Comparing Softdrop mass VS GloPart: 2p mass regression..

## Softdrop

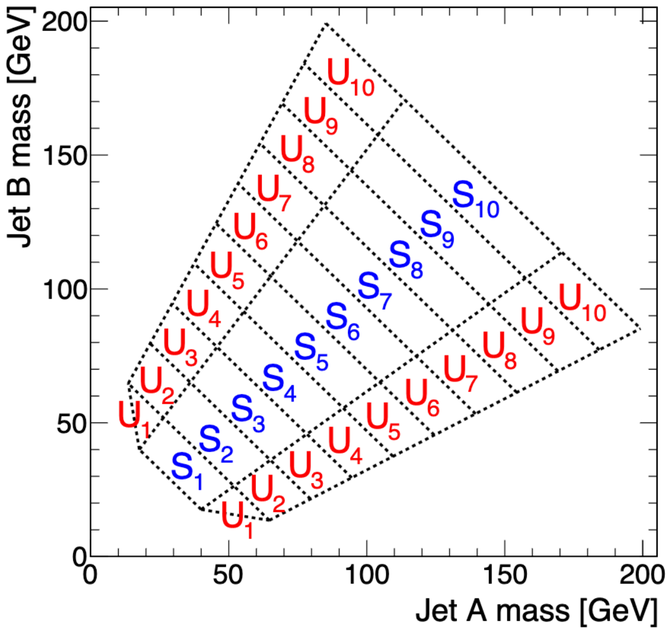
- Removes soft radiation
- Harsher grooming giving poor mass resolution as compared to GloPart.

## Glopart

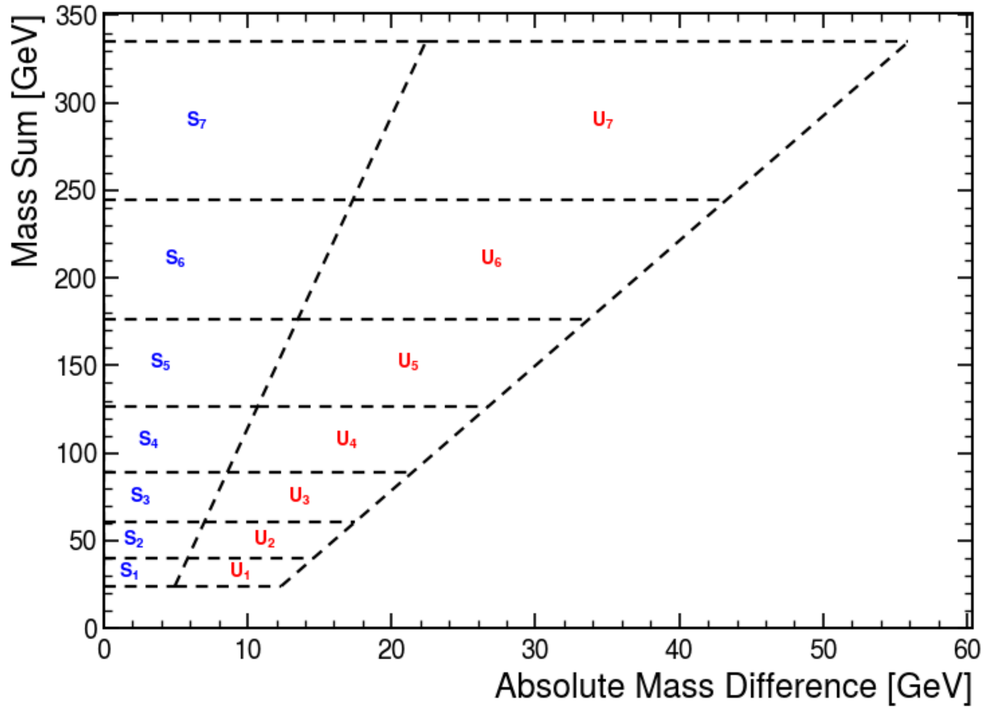
- Directly regresses jet mass
- Retains more information
- Significantly improves low-mass resolution.

# Signal extraction approach

Run 2 Approach




Run 3 Approach




- Signal concentrated near m_diff=0, Background spreads with more m_diff
- Easier to code and read.
- Provides a more natural separation of signal and background.

# Mass Grid Construction

Mass Point → Gaussian Fit ($m_{sum}$ && $m_{diff}$) → Extract σ

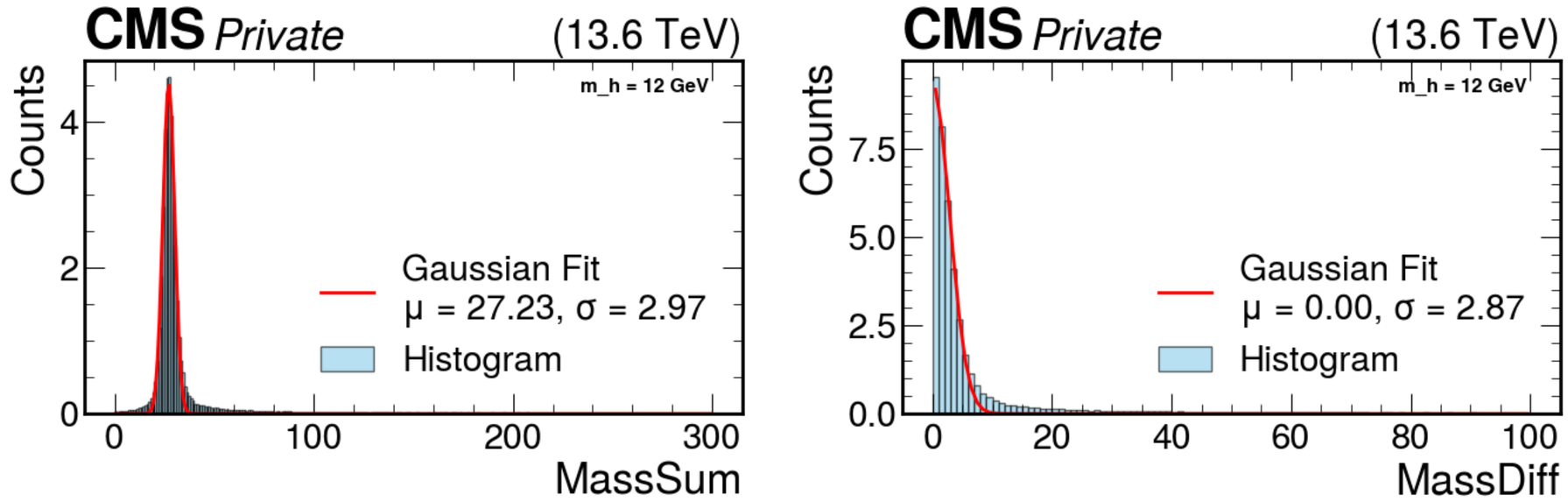
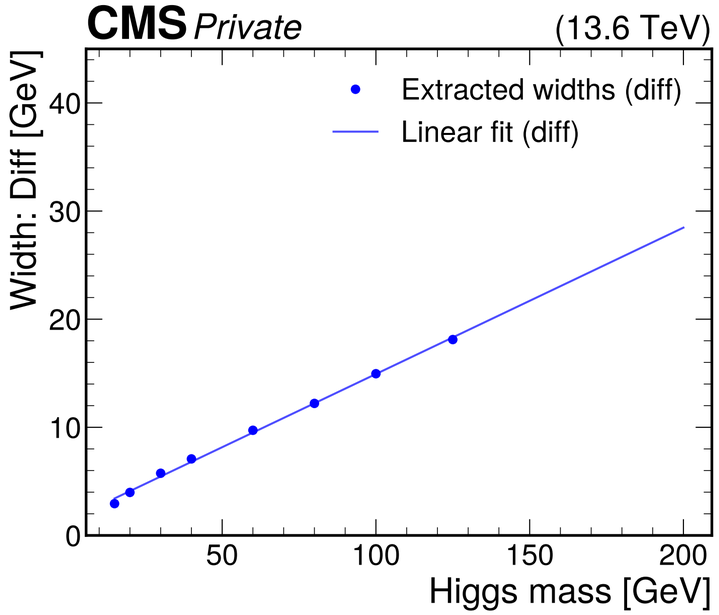



**Figure 5:** Gaussian fitted Mass Sum and Mass Difference distributions.

# Mass Grid Construction

Mass Point → Gaussian Fit ($m_{sum}$ && $m_{diff}$) → Extract σ → Linear fit



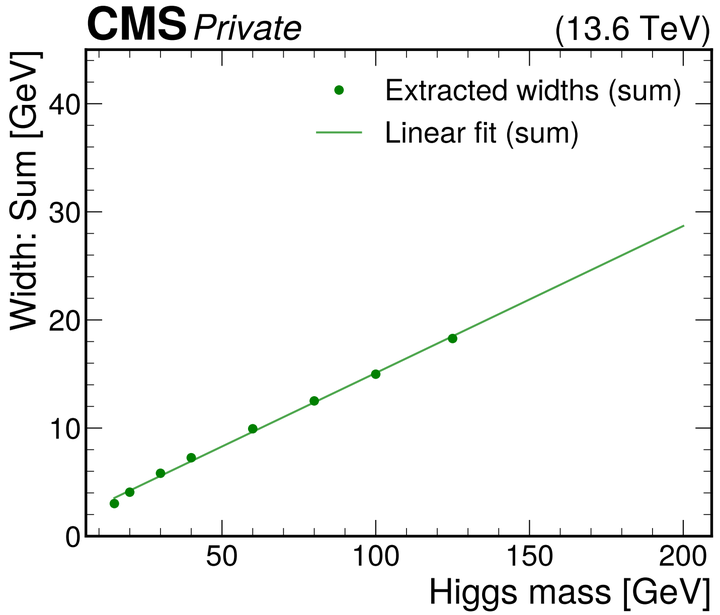




**Figure 6:** Linear fit for σ values for Mass Sum and Mass Difference distributions.

# Mass Grid Construction

Mass Point → Gaussian Fit ($m_{sum}$ && $m_{diff}$) → Extract σ → Linear fit → Define bins boundaries

$$m_{sum}^{i+1} = m_{sum}^{i} + 5 \cdot \sigma_{sum}^{i}$$

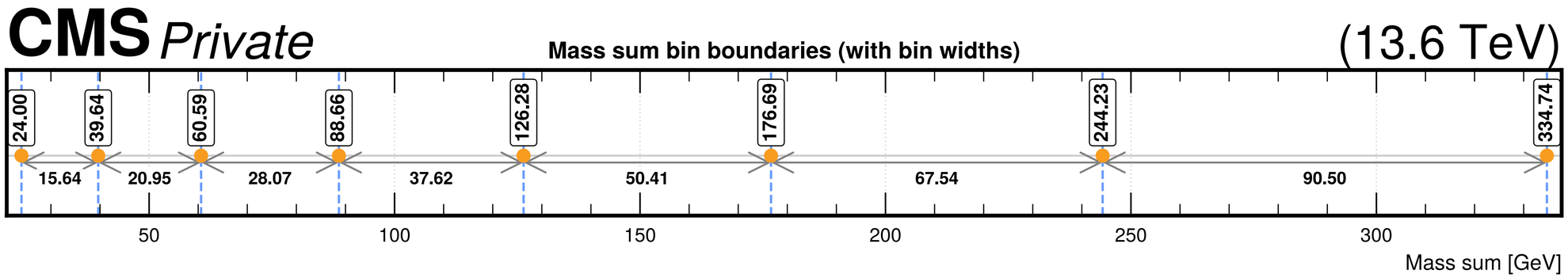



**Figure 7:** Mass Sum binning.

# Mass Grid Construction

Mass Point → Gaussian Fit ($m_{sum}$ && $m_{diff}$) → Extract σ → Linear fit → Define bins boundaries → Split S/U regions ($m_{diff}$)

$$m_{sum}^{i+1} = m_{sum}^{i} + 5 \cdot \sigma_{sum}^{i}$$

- Signal: mass_diff ∈ [0, 2σ]
- Upper: mass_diff ∈ [2σ, 5σ]

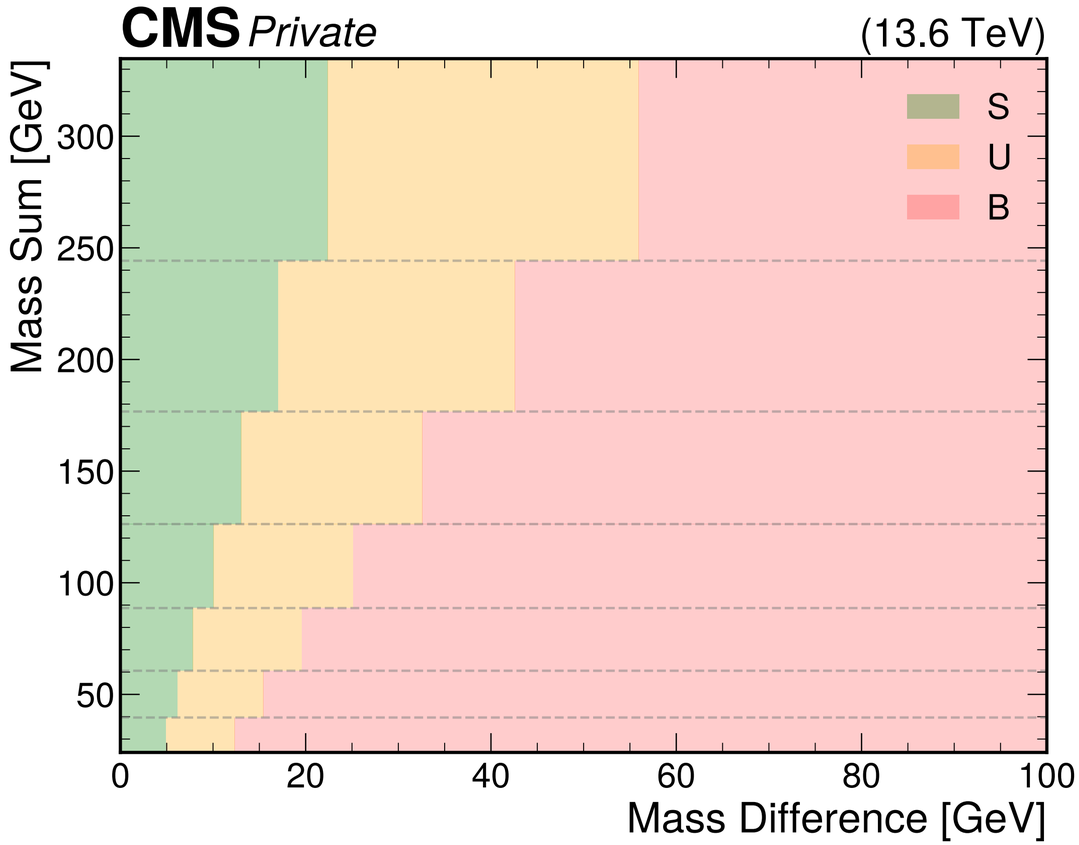



**Figure 8:** Final Mass Grid..

# Background estimation with ABCD method

| Regions | Definition |
|---|---|
| Tag (TR) | both jets with high b-tag score (sum > 1.5) |
| Control (CR) | both jets with low b-tag score ($\text{score}_{\text{both Jets}}$) < 0.5) |
| Validation (VR) | one medium-tagged jet (0.5 < sum < 1.5) |

Derive

$$TF = \frac{CR_{\text{search}}}{CR_{\text{sideband}}}$$

**Table 3:** ABCD region definition.

- Background estimate with ABCD method[7].
- Define regions: **CR, VR, TR** (b-tag score) with **search** and **sideband** bins (defined from the mass Grid)

# Background estimation

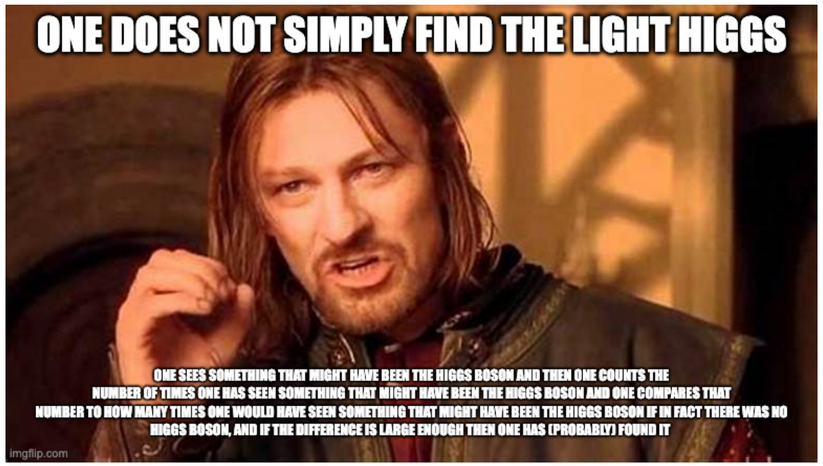
| Regions | Definition |
|---|---|
| Tag (TR) | both jets with high b-tag score (sum > 1.5) |
| Control (CR) | both jets with low b-tag score (sum < 0.5) |
| Validation (VR) | one medium-tagged jet |

Predict with the TF derived

$$N_{\text{exp,TR}} = TF \times TR_{\text{sideband}}$$

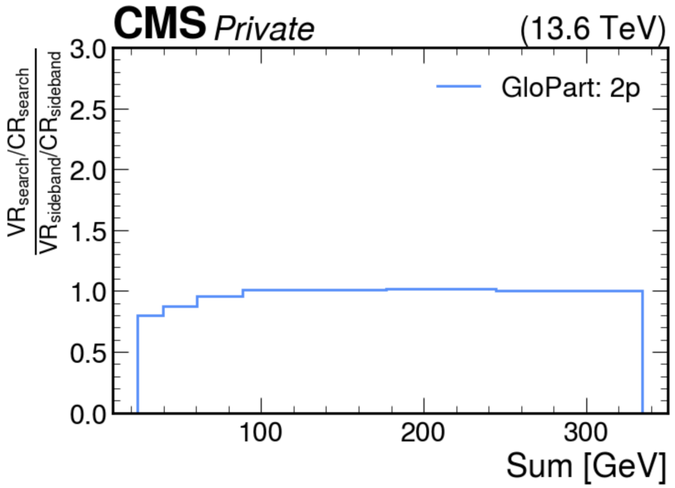
**Table 3:** ABCD region definition.

- Predict in validation/target regions
- Compare prediction vs observed in VR/TR



# ABCD Closure Test

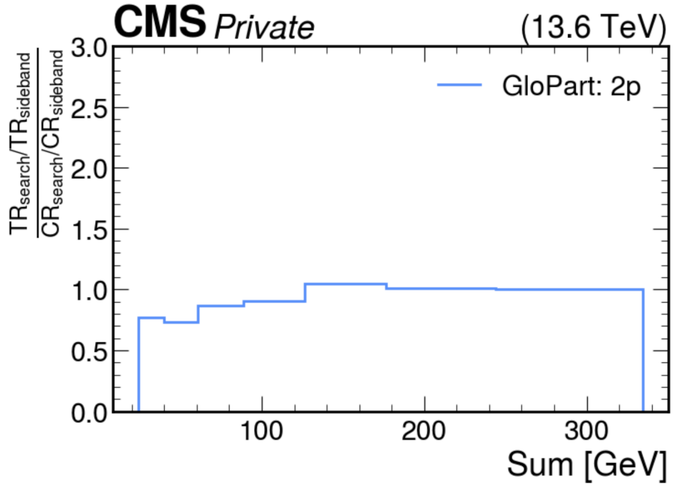
Validation Region




VR

| Bin | Range (Low–High) | Expected | Observed | % Difference |
|---|---|---|---|---|
| 0 | 24.0–39.6 | 65.12 ± 2.59 | 51.40 ± 1.35 | 26.69 ± 5.44 |
| 1 | 39.6–60.6 | 192.86 ± 2.34 | 166.59 ± 2.42 | 15.77 ± 1.89 |
| 2 | 60.6–88.7 | 314.55 ± 2.83 | 297.30 ± 3.24 | 5.80 ± 1.40 |
| 3 | 88.7–126.3 | 474.61 ± 3.39 | 472.58 ± 4.08 | 0.43 ± 1.12 |
| 4 | 126.3–176.7 | 642.59 ± 3.91 | 640.20 ± 4.75 | 0.37 ± 0.96 |
| 5 | 176.7–244.2 | 773.80 ± 4.32 | 779.67 ± 5.24 | 0.75 ± 0.87 |
| 6 | 244.2–334.7 | 798.21 ± 4.42 | 788.68 ± 5.27 | 1.21 ± 0.87 |

Tag Region

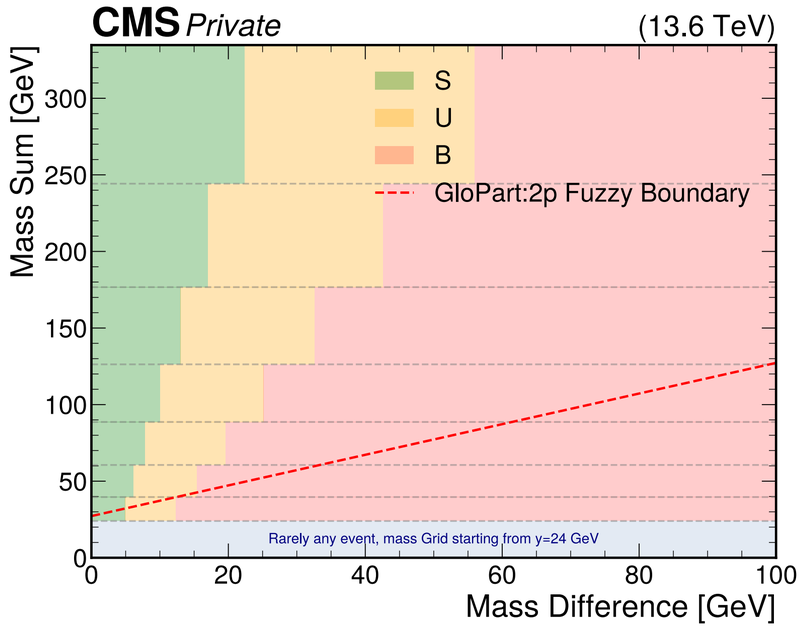


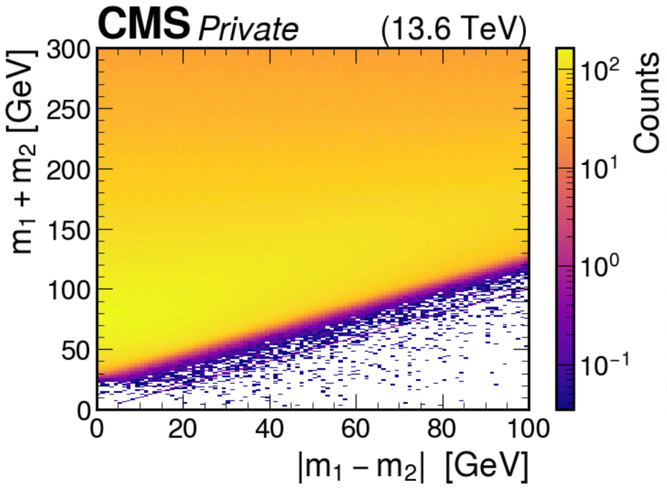

TR

| Bin | Range (Low–High) | Expected | Observed | % Difference |
|---|---|---|---|---|
| 0 | 24.0–39.6 | 2.29 ± 0.48 | 1.94 ± 0.26 | 18.17 ± 27.17 |
| 1 | 39.6–60.6 | 3.16 ± 0.30 | 2.53 ± 0.30 | 24.69 ± 15.03 |
| 2 | 60.6–88.7 | 2.91 ± 0.27 | 2.78 ± 0.31 | 4.57 ± 14.47 |
| 3 | 88.7–126.3 | 3.50 ± 0.29 | 3.49 ± 0.35 | 0.47 ± 12.97 |
| 4 | 126.3–176.7 | 4.67 ± 0.33 | 5.38 ± 0.44 | 13.26 ± 11.14 |
| 5 | 176.7–244.2 | 6.94 ± 0.40 | 7.71 ± 0.52 | 9.98 ± 9.15 |
| 6 | 244.2–334.7 | 8.78 ± 0.46 | 9.68 ± 0.58 | 9.25 ± 8.14 |

**Table 4:** ABCD closure test results for VR and TR..

# ABCD Closure Test




Tag Region

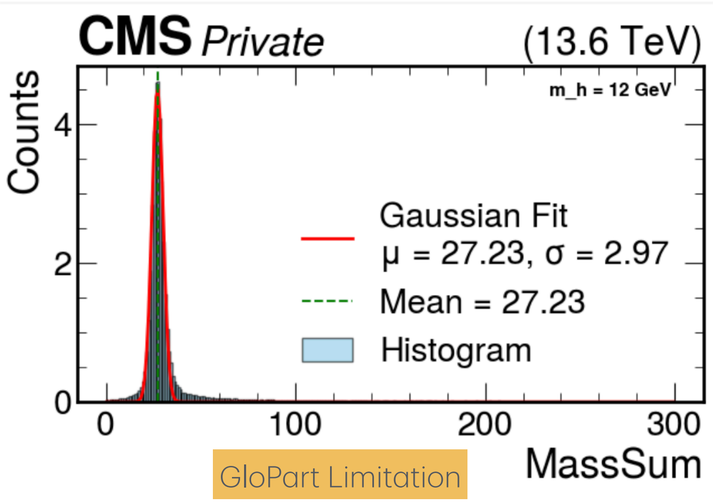
| Bin | TF |
|---|---|
| 0 | 2.23 |
| 1 | 0.67 |
| 2 | 0.66 |
| 3 | 0.66 |

VR

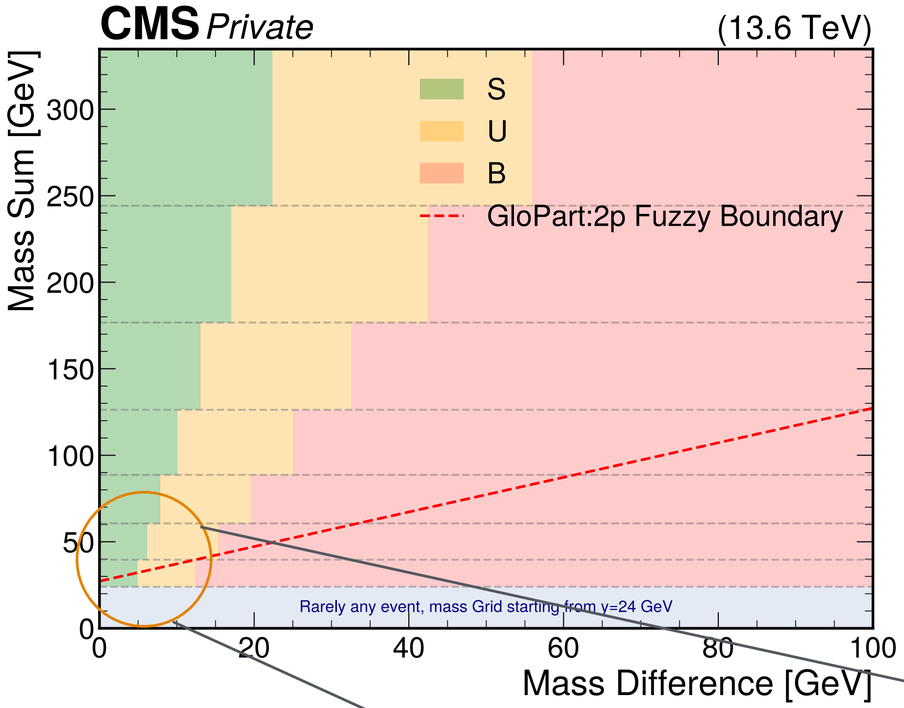
TR

| Bin | Range (Low–High) | Expected | Observed | % Difference |
|---|---|---|---|---|
| **0** | 24.0–39.6 | 2.29 ± 0.48 | 1.94 ± 0.26 | 18.17 ± 27.17 |
| **1** | 39.6–60.6 | 3.16 ± 0.30 | 2.53 ± 0.30 | 24.69 ± 15.03 |
| **2** | 60.6–88.7 | 2.91 ± 0.27 | 2.78 ± 0.31 | 4.57 ± 14.47 |
| **3** | 88.7–126.3 | 3.50 ± 0.29 | 3.49 ± 0.35 | 0.47 ± 12.97 |
| **4** | 126.3–176.7 | 4.67 ± 0.33 | 5.38 ± 0.44 | 13.26 ± 11.14 |
| **5** | 176.7–244.2 | 6.94 ± 0.40 | 7.71 ± 0.52 | 9.98 ± 9.15 |
| **6** | 244.2–334.7 | 8.78 ± 0.46 | 9.68 ± 0.58 | 9.25 ± 8.14 |

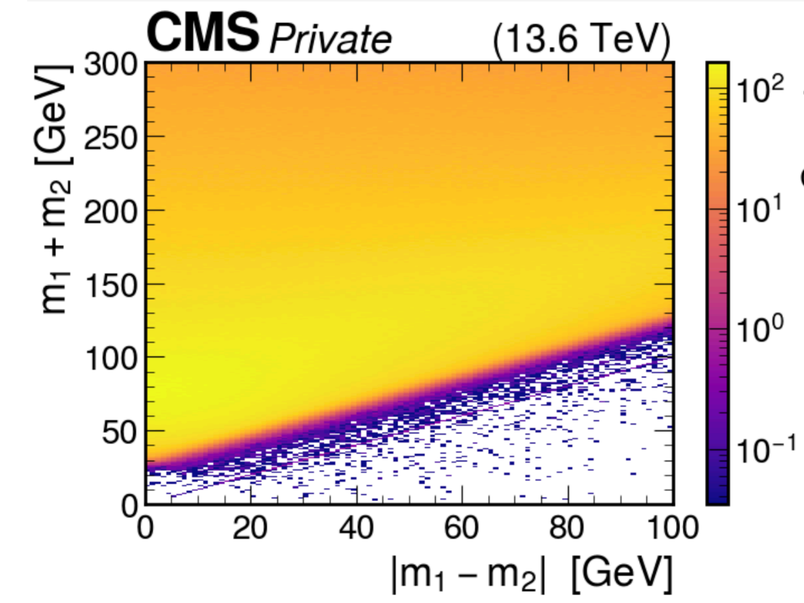
# GloPart:2p limitation

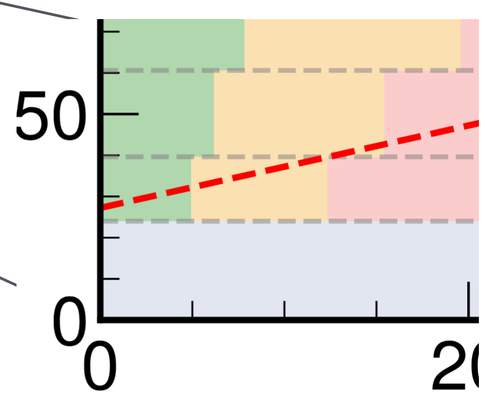



GloPart Limitation




Limitation shown in mass grid




| Bin | VR | TR |
|---|---|---|
| 1 | 2.82 | 2.23 |
| 2 | 0.78 | 0.67 |
| 3 | 0.7 | 0.66 |
| 4 | 0.67 | 0.66 |

Transfer Factor

**Figure 6:** GloPart limitation.

- GloParT training done on datasets with bb jet mass down to roughly mH=14 GeV

# Results

Before

Original: Over-predicting

| Bin | Range (Low–High) | TF | Exp (VR) | Obs (VR) | Exp (TR) | Obs (TR) | % diff (VR) | % diff (TR) |
|---|---|---|---|---|---|---|---|---|
| 0 | 24.0–39.6 | 2.8286 ± 0.0203 | 65.12 ± 2.59 | 51.40 ± 1.35 | 2.29 ± 0.48 | 1.94 ± 0.26 | 26.69 ± 5.44 | 18.17 ± 29.36 |
| 1 | 39.6–60.6 | 0.7872 ± 0.0016 | 192.86 ± 2.34 | 166.59 ± 2.42 | 3.16 ± 0.30 | 2.53 ± 0.30 | 15.77 ± 1.89 | 24.69 ± 18.77 |
| 2 | 60.6–88.7 | 0.7061 ± 0.0009 | 314.55 ± 2.83 | 297.30 ± 3.24 | 2.91 ± 0.27 | 2.78 ± 0.31 | 5.80 ± 1.40 | 4.57 ± 15.23 |
| 3 | 88.7–126.3 | 0.6721 ± 0.0007 | 474.61 ± 3.39 | 472.58 ± 4.08 | 3.50 ± 0.29 | 3.49 ± 0.35 | 0.43 ± 1.12 | 0.47 ± 13.05 |
| 4 | 126.3–176.7 | 0.6568 ± 0.0007 | 642.59 ± 3.91 | 640.20 ± 4.75 | 4.67 ± 0.33 | 5.38 ± 0.44 | 0.37 ± 0.96 | 13.26 ± 9.30 |
| 5 | 176.7–244.2 | 0.6639 ± 0.0007 | 773.80 ± 4.32 | 779.67 ± 5.24 | 6.94 ± 0.40 | 7.71 ± 0.52 | 0.75 ± 0.87 | 9.98 ± 8.02 |
| 6 | 244.2–334.7 | 0.6705 ± 0.0007 | 798.21 ± 4.42 | 788.68 ± 5.27 | 8.78 ± 0.46 | 9.68 ± 0.58 | 1.21 ± 0.87 | 9.25 ± 7.22 |

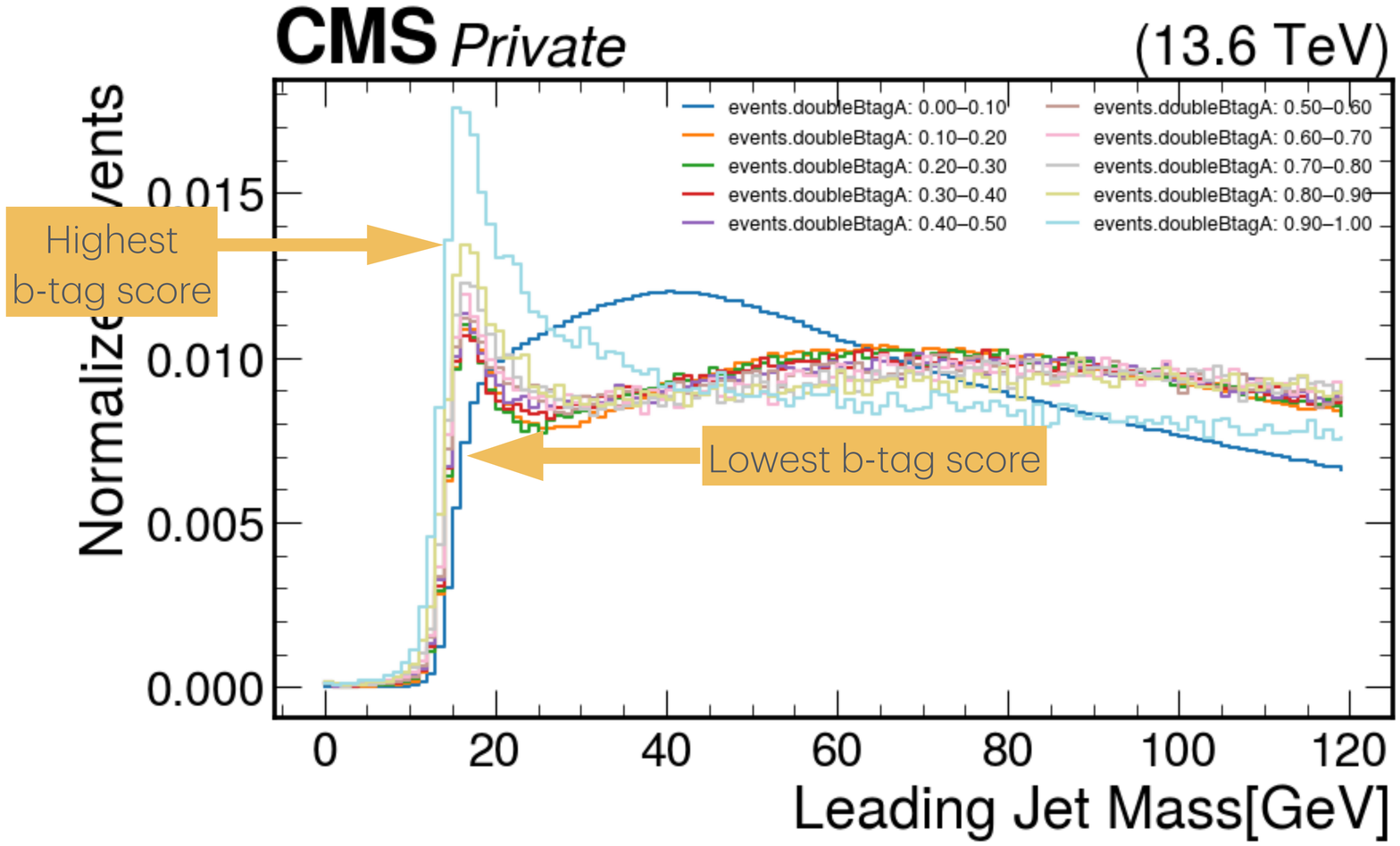
After

Updated: Under-predicting

| Bin | Range (Low–High) | TF | Exp (VR) | Obs (VR) | Exp (TR) | Obs (TR) | % diff (VR) | % diff (TR) |
|---|---|---|---|---|---|---|---|---|
| 0 | 24.0–39.6 | 0.1235 ± 0.0005 | 33.11 ± 0.40 | 51.40 ± 1.35 | 0.60 ± 0.05 | 1.94 ± 0.26 | 35.58 ± 4.14 | 69.24 ± 4.91 |
| 1 | 39.6–60.6 | 0.2338 ± 0.0004 | 161.44 ± 1.18 | 166.59 ± 2.42 | 1.90 ± 0.13 | 2.53 ± 0.30 | 3.09 ± 1.66 | 24.93 ± 10.13 |
| 2 | 60.6–88.7 | 0.2808 ± 0.0003 | 323.39 ± 1.83 | 297.30 ± 3.24 | 2.62 ± 0.16 | 2.78 ± 0.31 | 8.77 ± 1.17 | 5.81 ± 12.07 |
| 3 | 88.7–126.3 | 0.3069 ± 0.0003 | 516.94 ± 2.42 | 472.58 ± 4.08 | 3.78 ± 0.20 | 3.49 ± 0.35 | 9.39 ± 0.94 | 8.46 ± 12.35 |
| 4 | 126.3–176.7 | 0.3186 ± 0.0003 | 683.14 ± 2.84 | 640.20 ± 4.75 | 5.60 ± 0.25 | 5.38 ± 0.44 | 6.71 ± 0.82 | 3.94 ± 9.61 |
| 5 | 176.7–244.2 | 0.3480 ± 0.0003 | 819.88 ± 3.25 | 779.67 ± 5.24 | 8.20 ± 0.32 | 7.71 ± 0.52 | 5.16 ± 0.76 | 6.31 ± 8.28 |
| 6 | 244.2–334.7 | 0.6705 ± 0.0007 | 798.21 ± 4.42 | 788.68 ± 5.27 | 8.78 ± 0.46 | 9.68 ± 0.58 | 1.21 ± 0.87 | 9.25 ± 7.22 |

**Table 5:** Updated ABCD closure test results for VR and TR..

# Underlying issue



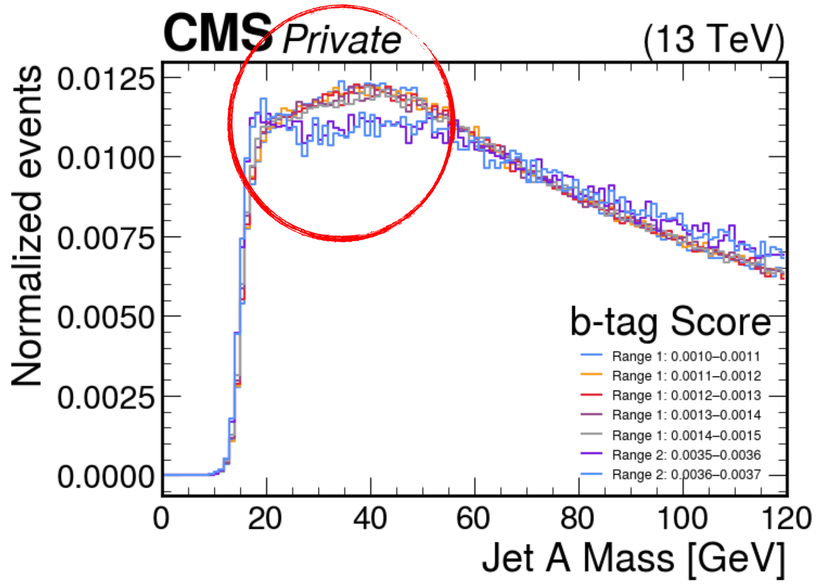




**Figure 7:** Regressed mass dependance on b-tag score.

- Mass Distribution changes with b-tag score values.

- The mass distribution for deriving TF (CR) is different than its used in. (TR and VR)

# Updated ABCD closure

Original

| Bin | Edges | TF | Exp (VR) | Obs (VR) | Exp (TR) | Obs (TR) | % diff (VR) | % diff (TR) |
|---|---|---|---|---|---|---|---|---|
| 0 | 24.0 – 39.6 | 2.8276 ± 0.0203 | 58.93 ± 2.34 | 46.31 ± 1.21 | 2.06 ± 0.43 | 1.77 ± 0.24 | 27.24 ± 5.45% | 16.02 ± 28.75% |
| 1 | 39.6 – 60.6 | 0.7874 ± 0.0016 | 174.05 ± 2.11 | 150.75 ± 2.19 | 2.92 ± 0.27 | 2.25 ± 0.27 | 15.46 ± 1.88% | 29.82 ± 19.53% |
| 2 | 60.6 – 88.7 | 0.7058 ± 0.0009 | 284.08 ± 2.55 | 268.77 ± 2.92 | 2.59 ± 0.24 | 2.47 ± 0.28 | 5.70 ± 1.40% | 4.98 ± 15.37% |
| 3 | 88.7 – 126.3 | 0.6722 ± 0.0007 | 429.00 ± 3.06 | 427.33 ± 3.68 | 3.22 ± 0.26 | 3.17 ± 0.32 | 0.39 ± 1.12% | 1.50 ± 13.09% |
| 4 | 126.3 – 176.7 | 0.6567 ± 0.0007 | 579.59 ± 3.52 | 577.95 ± 4.28 | 4.22 ± 0.30 | 4.84 ± 0.39 | 0.28 ± 0.96% | 12.85 ± 9.33% |
| 5 | 176.7 – 244.2 | 0.6639 ± 0.0007 | 697.95 ± 3.89 | 702.84 ± 4.72 | 6.29 ± 0.36 | 7.10 ± 0.47 | 0.70 ± 0.87% | 11.40 ± 7.83% |
| 6 | 244.2 – 334.7 | 0.6705 ± 0.0007 | 719.28 ± 3.98 | 709.71 ± 4.74 | 7.99 ± 0.41 | 8.77 ± 0.53 | 1.35 ± 0.87% | 8.95 ± 7.21% |

Updated

| Bin | Edges | TF | Exp(VR) | Obs(VR) | Exp(TR) | Obs(TR) | %diff(VR) | %diff(TR) |
|---|---|---|---|---|---|---|---|---|
| 0 | 24.0 - 39.6 | 2.2147±0.2331 | 46.15±5.18 | 46.31±1.21 | 1.61±0.38 | 1.77±0.24 | 0.34±11.49 % | 9.12±24.46 % |
| 1 | 39.6 - 60.6 | 0.6998±0.0315 | 154.69±7.20 | 150.75±2.19 | 2.59±0.27 | 2.25±0.27 | 2.62±4.98 % | 15.39±18.12 % |
| 2 | 60.6 - 88.7 | 0.7042±0.0209 | 283.45±8.79 | 268.77±2.92 | 2.59±0.25 | 2.47±0.28 | 5.46±3.43 % | 4.74±15.65 % |
| 3 | 88.7 - 126.3 | 0.7026±0.0150 | 448.39±10.07 | 427.33±3.68 | 3.36±0.28 | 3.17±0.32 | 4.93±2.50 % | 6.08±13.86 % |
| 4 | 126.3 - 176.7 | 0.6724±0.0122 | 593.44±11.33 | 577.95±4.28 | 4.32±0.31 | 4.84±0.39 | 2.68±2.09 % | 10.76±9.69 % |
| 5 | 176.7 - 244.2 | 0.6659±0.0114 | 700.09±12.59 | 702.84±4.72 | 6.31±0.38 | 7.10±0.47 | 0.39±1.91 % | 11.13±8.00 % |
| 6 | 244.2 - 334.7 | 0.6687±0.0116 | 717.39±13.08 | 709.71±4.74 | 7.97±0.43 | 8.77±0.53 | 1.08±1.96 % | 9.19±7.36 % |

**Table 6:** Updated ABCD closure test results for VR and TR..

# Summary

- Revisited light Higgs search using new Run-3 tools.
- Run-2 relied on SoftDrop mass and BDT Hbb tagging.
- Run-3 uses GloParT tagging and mass regression optimized for two-prong resonances.
- New mass grid provides improved signal/background separation.
- Data-driven ABCD method validated over most of phase space.
- Ongoing studies aim to demonstrate that the current low-mass limitation primarily from GloParT training (mH ~ 14 GeV), while the analysis methodology remains valid.


Thank You!

# References


1. U. Ellwanger, C. Hugonie, A.M. Teixeira, The Next-to-Minimal Supersymmetric Standard Model, **Phys. Rep. 496 (2010) 1–77**, doi:10.1016/j.physrep.2010.07.001.
2. G.C. Branco et al., Theory and phenomenology of two-Higgs-doublet models, **Phys. Rep. 516 (2012) 1–102**, doi:10.1016/j.physrep.2012.02.002.
3. ATLAS Collaboration, Search for additional Higgs bosons in the context of the MSSM and other models, recent Run-2 combination papers.
4. CMS Collaboration, Searches for additional Higgs bosons beyond the Standard Model, Run-2 combinations.
5. U. Ellwanger, C. Hugonie, A.M. Teixeira, The Next-to-Minimal Supersymmetric Standard Model, **Phys. Rep. 496 (2010) 1–77**, doi:10.1016/j.physrep.2010.07.001.
6. Global Particle Transformer, https://cds.cern.ch/record/2904879/files/HIG-23-012-pas.pdf